Cogent Engineering

ISSN: (Print) (Online) Journal homepage: www.tandfonline.com/journals/oaen20

Dispersion of gamma dose rates and natural radionuclides in the coastal environments of the Unumherin community in Niger Delta

Maxwell Omeje, Godfrey Usiaka Aimua, Olusegun Oladotun Adewoyin, Muyiwa Michael Orosun, Emmanuel Sunday Joel, Mojisola Rachael Usikalu, Omohinmin A. Conrad, Oha I. Andrew, Benjamin Nnamdi Ekwueme, Nwankwo Chukwuma Michael & Omeje U. Anne

To cite this article: Maxwell Omeje, Godfrey Usiaka Aimua, Olusegun Oladotun Adewoyin, Muyiwa Michael Orosun, Emmanuel Sunday Joel, Mojisola Rachael Usikalu, Omohinmin A. Conrad, Oha I. Andrew, Benjamin Nnamdi Ekwueme, Nwankwo Chukwuma Michael & Omeje U. Anne (2023) Dispersion of gamma dose rates and natural radionuclides in the coastal environments of the Unumherin community in Niger Delta, Cogent Engineering, 10:1, 2204546, DOI: 10.1080/23311916.2023.2204546

To link to this article: https://doi.org/10.1080/23311916.2023.2204546

Published online: 01 Jun 2023.

Omeje et al., *Cogent Engineering* (2023), 10: 2204546
https://doi.org/10.1080/23311916.2023.2204546

cogent engineering

ENVIRONMENTAL ENGINEERING | RESEARCH ARTICLE

Dispersion of gamma dose rates and natural radionuclides in the coastal environments of the Unumherin community in Niger Delta

Maxwell Omeje[1]*, Godfrey Usiaka Aimua[1], Olusegun Oladotun Adewoyin[1], Muyiwa Michael Orosun[2], Emmanuel Sunday Joel[3], Mojisola Rachael Usikalu[1], Omohinmin A. Conrad[4], Oha I. Andrew[5], Benjamin Nnamdi Ekwueme[6], Nwankwo Chukwuma Michael[7] and Omeje U. Anne[8]

Received: 16 October 2022
Accepted: 01 April 2023

*Corresponding author: Maxwell Omeje, Department of Physics, College of Science and Technology, Covenant University, KM 10, Idiroko Road, Ota, Ogun State
E-mail: maxwell.omeje@covenantuniversity.edu.ng

Reviewing editor:
Sanjay Kumar Shukla, School of Engineering, Edith Cowan University, Australia

Additional information is available at the end of the article

Abstract: The outdoor gamma dose rates and the activity concentrations of potassium-40, uranium-238, and thorium-232 within the study area were carried out using calibrated hand-held gamma detector (RS-125 gamma spectrometer) and NaI(Tl) gamma spectroscopy. The in-situ measurement results of the gamma dose rate indicate that the hotspot is at location 4 with a value of 100 nGyh-1. The results from the NaI(Tl) gamma detector revealed the highest activity concentrations of potassium-40, uranium-238, and thorium-232 to be 288.09, 96.49, and 136.12 $Bqkg^{-1}$ for sediments and 257.31, 66.93, and 96.57 Bqkg for water, respectively. The highest mean activity concentration of potassium-40 and uranium-238 was observed in Catfish with values of 151.87 and 38.00 $Bqkg^{-1}$, whereas the highest value for the activity of thorium-232 was observed in Tilo Fish with a value of 89.02 Bqkg-1. In comparison, all the observed values are higher than the population-weighted average of 420.00, 32.00, and 45.00 $Bqkg^{-1}$ for potassium-40, uranium-238, and thorium-232 according to UNSCEAR. Geologically, this may be attributed to the marine incursion of regional tectonic subsidence during transgression. Statistically, the correlation results confirmed that the enhanced outdoor dose rates at the coastline environment were caused mainly by uranium-238, followed by thorium-232 and then potassium-40 in magnitude. The mean hazard indices calculated for the samples were also observed to be within the global average values recommended by ICRP.

Subjects: Environmental Studies; Environmental Management; Environmental Issues; Environment & Health; Ecology - Environment Studies; Environmental Change & Pollution

Keywords: gamma spectroscopy; catfish; Niger Delta; radiological; cancer risk; sediments

1. Introduction

There is widespread degradation of the environment of the Niger Delta region of Nigeria such that the United Nations Environment Program described it as an ecological wasteland (Babatunde et al., 2019). The contamination is due mainly to unregulated oil and gas production activities leading to oil spills and illegal disposal of contaminated materials, and indiscriminate industrial

and domestic discharges into water bodies. This widespread contamination includes naturally occurring radioactive materials (NORM) and technologically enhanced radioactive materials (TENORM) (Babatunde et al., 2019). The Niger Delta region is the hub of oil and gas activities, providing huge employment and socio-economic benefits to its indigenes and accounting for more than 90% of foreign exchange earnings for the country (Nigeria). However, uncontrolled spills and discharges from these activities have left the land desolate, degrading most of its aquifers and surface waters, leaving the indigenes with a Hobson choice, eating, and drinking contaminated substances every day of their lives (Babatunde et al., 2019).

Radionuclides and their effects on the coastal environment are the topics of research in environmental radioactivity research (Zakaly et al., 2021). Both artificial and natural radiation sources can be transported over long or short distances in various ways within the environment (Zakaly et al., 2021).

Human beings are exposed to natural radiation from external sources, such as sediment radionuclides, cosmic radiation, and the inner radiation of the body by radionuclides (Abbasi et al., 2021). Among the different radiation sources, natural radiation is the most considerable source of overall exposure to humans and the ecosystem (Fallah et al., 2019). Marine sediments play an important role in offering vital information when measuring environmental and geochemical contamination compared to other potential natural radioactivity sources (Janadeleh, Jahangiri, et al., 2018; Janadeleh, Kameli, et al., 2018). However, it has been revealed that sediment is an important bed of contamination and a potential contamination source in aquatic environments (Pappa et al., 2016). The Niger Delta ecosystem contains one of the highest concentrations of biodiversity on the planet and in addition to supporting abundant flora and fauna, its arable terrain and water resources can sustain a wide variety of crops, lumbar, and agricultural trees, and more species of freshwater fisheries than any other wetland in West Africa. This incredible ecosystem is, however, vulnerable to destruction by petroleum and its products due to oil industry activities within the area (Ajao & Anurigwo, 2002).

In coastal environments such as Niger Delta, sediments play a dominant role in hydrous radioecology in environmental radioactivity measurements (Abbasi et al., 2020). These naturally occurring radionuclides emigrate from the lithosphere to broader natural ecosystems through the erosion of terrestrial rock and subsequent transport via water, wind, and gravity (Abbasi et al., 2021; Zakaly et al., 2021). The exploitation and exploration of crude oil and gas may bring economic benefits to a country, but its activities are destructive to the environment even at the safest and best-operating practices and such unsafe acts may include the redistribution of naturally occurring radioactive materials (NORM) (Ajao & Anurigwo, 2002; Babatunde et al., 2019). The radioactivity concentration and heavy metal pollutants in the marine environment have been revealed as severe pollution concerns. These elements attach to particles in marine ambiance and further accumulated in the sediments (Abbasi et al., 2020). The sources of these elements in the marine environment can be either anthropogenic such as industrial activity and mining (Papaefthymiou et al., 2007) or the natural ingredient of the Earth's crust that is present in all the terrestrial ecosystems (Uluturhan et al., 2011). These isotopes are widely distributed in the earth's environment occurring in trace amounts (ppm/ppb) in sediments, seafood, air, soil, foodstuff, surface, and groundwater (Pates & Mullinger, 2007). The extent of distribution depends on the geological features of the area, the industrial application of radionuclides, and the chemical and biochemical distribution of ^{238}U and ^{232}Th and their progenies. Also widely distributed is ^{40}K, a natural radioactive isotope occurring in high background levels in biological systems and earth minerals such as rocks, clay, shale, limestone, and granite.

Consequently, these naturally occurring radionuclides enter the food chain through the ingestion of marine foods (Abbasi et al., 2020; Hurtado-Bermúdez et al., 2019). Several studies reported measured natural radioactivity in the sediments of the Mediterranean Sea (Delbono et al., 2016; Fouskas et al., 2018; Radi Dar & El-Saharty, 2012). They have always been existing in seawater and

sediments, but the high concentration observed in some sea creatures such as fish is possible due to the discharge of industrial waste containing pollutants into the marine environment (Ananias et al., 2022; Zakaly et al., 2021). On the other hand, several studies have been widely studied on the heavy metal pollution in the Mediterranean Sea (Bastami et al., 2015; Bonsignore et al., 2018; Gu et al., 2017; Nour et al., 2019; Tiphaine et al., 2018; Zaqoot et al., 2018). During the processes of crude oil and gas recovery from the earth's crust, naturally occurring radioactive materials (NORM) associated with the minerals in the earth's crust are brought to the surface and distributed widely in the environment with potential consequences of contaminating food and water sources consumed by humans (Jonkers et al., 1997), and the International Association of Oil and Gas Producers (International Association of Oil and Gas Producers OGP, 2008) noted that during the production process, NORM now referred to as TENORM (technologically enhanced natural occurring radioactive materials) flows with the oil, gas, and water mixture and accumulates in scale, sludge, and scrapings. Several studies have linked the susceptibility of certain aquatic microorganisms to all kinds of pollution and revealed that microbiological assessment can be used as indices to diagnose soil heavy metal pollution (Savvaidis et al., 2001; Tang et al., 2019; Wang et al., 2018). These studies have been used for different sediment-water quality assessments in marine environments at different locations across the world. The unifying factor among the listed studies is their ability to uniquely provide information on the status of naturally occurring radioactivity and microbiological activity in marine sediments, which is the aim of these studies.

In Nigeria, data related to environmental radioactivity and marine sediment are very scanty. In cases where data are available, most of these studies undertaken were on soil radioactivity or are limited to selected geographical locations. Environmental radioactivity has not been carried out on the radiological and microbiological activity in the marine environment of Niger Delta, South-South Nigeria. In addition, the radiological parameters such as radium equivalent activity (Raeq), absorbed dose rate (D), external hazard index (Hex), representative-level index (Iγ), annual effective dose equivalent (AEDE), effective dose (Dorgan) on various organs and tissues, annual gonadal dose equivalent (AGDE), and excess lifetime cancer risk (ELCR) values have been evaluated. Finally, the radionuclides-microbial soil synergy that relies upon the chemical form of the elements and different soil features, including the mineralogical contents will be identified.

1.1. Geographical location and the geology of the study area

The Niger Delta Basin is an extension of the rift basin located in the Niger Delta and the Gulf of Guinea and lies in the southwestern part of the larger tectonic structure called the Benue Trough. It is located on the passive continental margin near the western coast of Nigeria. The volcanic Cameroon line and the passive continental margin bound the other side. It is proven or suspected to have access to Equatorial Guinea, Cameroon and São Tomé, and Príncipe. The basin is complex and carries a very high economic value containing a rich productive hydrocarbon system. The basin is one of the largest subaerial basins in Africa. The sediment fill has a depth ranging between 9 and 12 km and is composed of different geologic formations, which indicates the possibility of the formation of the basins. It also indicates the large-scale and regional tectonics of the area, with an extensional basin surrounded by many other basins formed from similar structure processes. The study area covers two communities in Warri Area in the Niger Delta as shown in Figure 1. They are the Unumherin and Okirigwe communities in the Delta State of Nigeria.

The geology of Niger Delta covers about 256,000 km. Initially, it was the older transgressive Paleocene prodelta that was built, which was Delta construction, and proceeded in discrete mini basins (Adegoke et al., 2017). These mini basins range in tectonic configuration from extensional through translational to compressional toe-thrust region. The Niger Delta outcropping units are Imo Formation and the Ameki Group. The Ameki group includes the Ameki, Nanka, Nsugbe, and Ogwashi-Asaba formation. The lithostratigraphic sequence of the subsurface units is as follows: major transgressive marine Akata shales, the petroliferous paralic Agbada Formation, and the continental Benin Sands (Adegoke et al., 2017; d'Almeida et al., 2016). The crude oil in the Niger

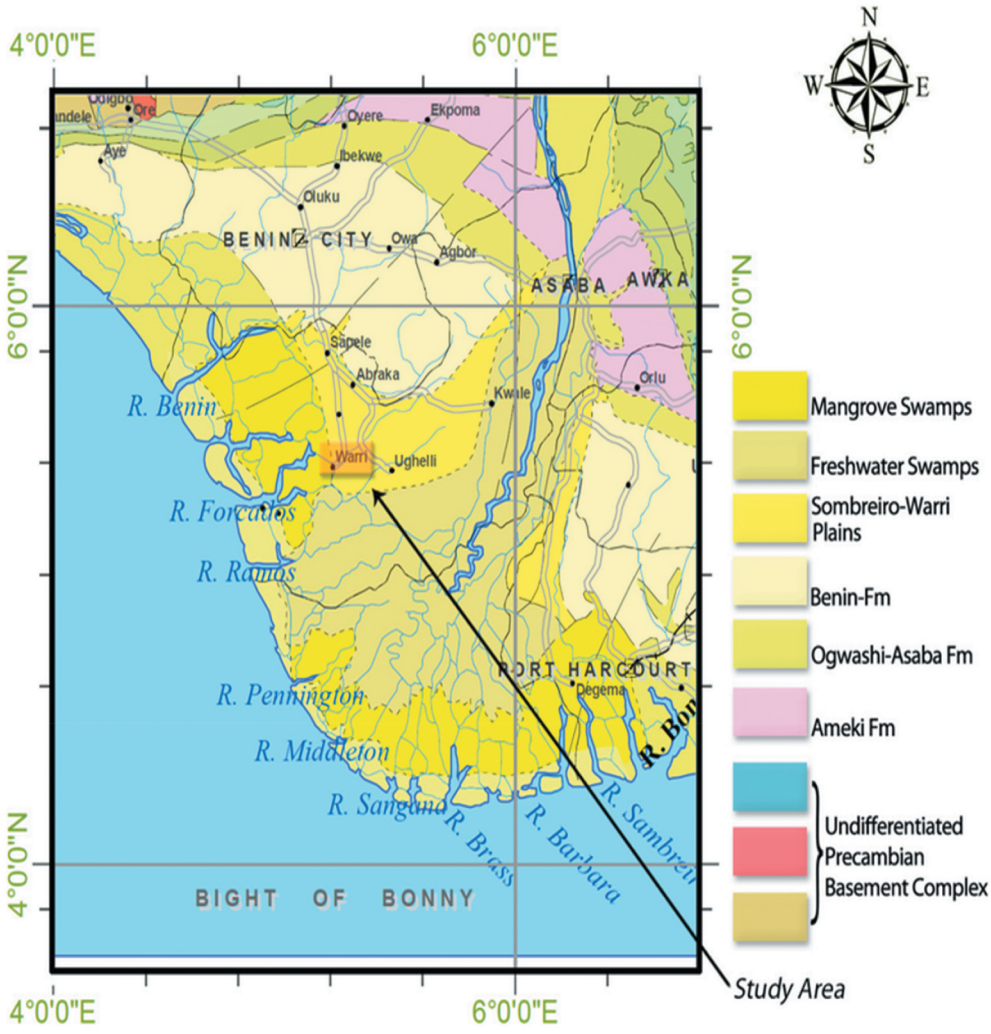

Figure 1. Geology of the study area.

Source: NGGSA, 2004 and Irwin, 2015

Delta has a low amount of sulfur, nickel-bearing, light waxy, and nongraded. The location and geology of the study area are shown in Figure 1.

The delta sequence comprises an upward-coarsening regressive association of the Tertiary clastic of up to 12 km thick. It is divided into three gross lithofacies: (1) marine shale and clay stones of unknown thickness at the base, (2) alterations of clay stones, sandstones, and siltstones, of which the percentage increase of sand is upwards, and (3) the alluvial sand is on the top. The stratigraphy and the Delta structure are intimately related. Each of the developments is being dependent on the interplay existing between the subsidence rates and sediment supply. The most dominant structures of the subsurface are post- and sync-sedimentary lithic normal faults, which can affect the main sequence of the delta.

1.2. The coastline sediments of the Atlantic coast of Unumherin community and Ethiope river

The nature of the Atlantic coast of the Unumherin community and the Ethiope river sediments shows some parts where communities have access to the Atlantic Ocean and Ethiope River for fishing and fetching water for domestic purposes (Omeje et al., 2020). They are parallel to the coastline sediments of other Atlantic coastal regions of Escravos, Forcados, Burutu, and Agbaro, which are located about some kilometers away from the Unumherin community and Ethiope river. The deposits from the Atlantic Ocean and Ethiope river comprise mudflats, salt marsh, and inner sandy flats. Within the Ocean and river sub-

environments, it cuts across the creeks and the bordering areas. Surface features such as vegetation, an association of different sediments, sedimentary structures, and textures, characterize the sub-environments along the coastal region and rivers. The sediments contain high contents of iron, phosphate, nitrate, and sulfates (Omeje, Emmanuel, et al., 2018). The tidal water along the ocean and river decreases its capacity towards the intertidal zone, and this increases the sediment deposits and reduces the size of the grains. These processes seem to be modified by the secondary agents caused by waves for rearrangements of the sediments in the study area.

2. Materials and methods

2.1. In situ gamma spectroscopy measurements using Super-Spec RS-125 gamma spectrometer

The in-situ measurement of the background gamma dose rates and the activity concentration of K-40, Th-232, and U-238 were carried out about 1 meter above the ground surface using a Super-SPEC RS-125 gamma detector coated with 2.0 cm x 2.0 cm NaI crystal. To accurately measure the levels of radioactivity going on in the sediment samples, the procedure (Omeje et al., 2020) was adopted. A portable hand-held radiation detector (Super-SPEC RS-125) from Canadian Geophysical Inc. was used to measure the background gamma dose level in the study area. This instrument is most suitable for detecting naturally occurring radionuclides and dose exposure. The equipment has a high degree of accuracy with uncertainty of ±5% at energies above 500 keV. Due to the sensitivity of the response at low energies to the individual detectors' characteristics, it can be used below 200 keV. The portable equipment has an incorporated design and direct assay read-out values, and the storage data point with weather protection is easy to use and highly sensitive. At each station, four different measurements were taken, and the average obtained was used to represent the actual data point for that site. At each point of measurement, the sediment sample was collected for laboratory gamma-ray spectroscopy counting. The background measurement was provided by the assay mode of RS-125 Super-SPEC, and dose rate data were directly acquired in nGy/h (Omeje et al., 2020). The measured data are stored in an Excel sheet with proper coordinates processed, georeferenced, and interpolated using ArcGIS (version 10.8) spatial analysis. Figure 2 presents the results of the ArcGis spatial distribution of dose rates measured in the study area.

2.2. Method of GIS analysis of background dose rates data samples measured in the study area

The spatial distribution of gamma dose rates in the coastal environments was carried out using an interpolated scheme of the inverse distance weighting interpolation function being applied to all the surveyed areas. The interpolated functions were used as input to ArcGIS 10.8.

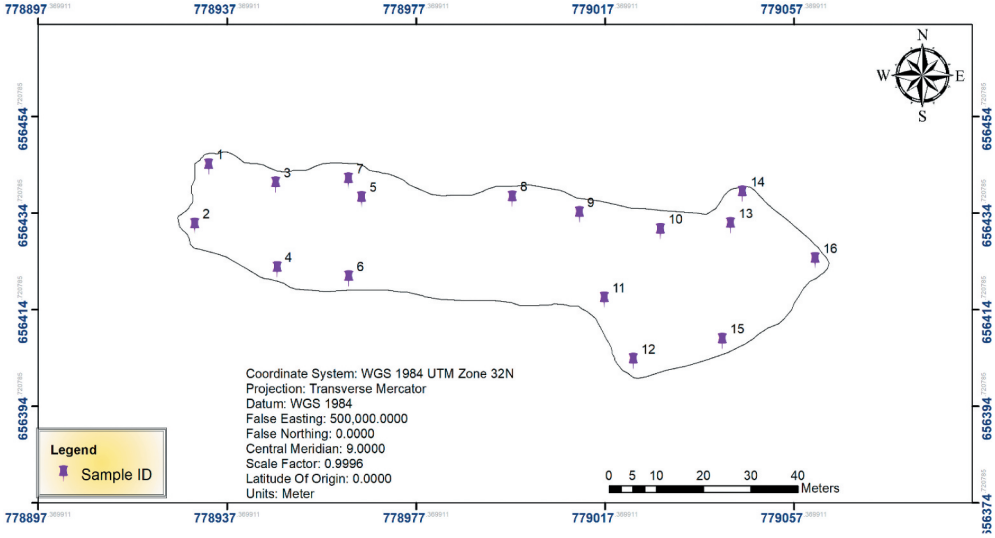

Figure 2. The sample collection points.

2.3. Sample collection and preparation of soil sediments, water, and fishes for laboratory gamma-ray spectrometry measurements

A total number of 16 samples from sediments, water, and 5 different species of fish were collected randomly within the selected coastal environments in the Warri Area of the Niger Delta. This was done in accordance with IAEA guidelines on the collection of soil samples for analysis (Omeje, Adewoyin, et al., 2018). They were obtained from the specified areas of the Unumherin Community between February 8 and 14, 2021, and the locations are shown in Figure 2. A minimum distance of 20 meters was maintained between two sampling points, and black polythene bags were used for the packing, taped up and marked according to the location, and together with a designated site code and coordinates of the sample. The samples were scooped at a depth between 10 and 50 cm (vertical distance) using a hand trowel. In the Unumherin Community, 15 different sediment samples were collected at the stations of the measured in-situ background gamma measurements, and a sample outside the study area was used as a control to sum it up to 16 sediment samples altogether. The samples were taken to Covenant University Microbiology Laboratory, where macroscopic traces of stones, rubbers, glass, plastic, animal and plant matter, and other large particles were removed to make sure the materials to be analyzed do not contain such impurities. The samples of sediments and fishes were air-dried at room temperature of about 29°C, for 3 days to reduce the mass contribution of water and to prevent any chemical reaction. The dried samples were later crushed using a ball mill to reduce the particle size and subsequently further dried in an electric oven at a temperature of 110 ± 1°C for 24 hours to completely remove any remnant moisture and obtained constant weight. Water samples were collected in high-density polyethylene containers at the same sampling site, which was previously washed in a solution of 10% nitric acid for 15 minutes, followed by repeated rinsing with distilled water and finally rinsing with ultrapure water (resistivity of about 18 MΩ cm^{-1}). The containers used for the collection were kept in sealed polyethylene bags before the collection of samples. To prevent it from contaminating the wall of the container, the water samples were stabilized with 5 ml of nitric acid in each liter of water.

2.4. Sample preparation/calibration of detector for gamma spectroscopy analysis

The soil samples were collected into a very clean polythene bag and well labeled to avoid mixing up of samples. The samples were transported to the Centre for Environmental Research Laboratory, Ahmadu Bello University, Zaria. The collected samples were dried at ambient temperature until there was no noticeable change in the mass of the sample. The dried samples were carefully crushed, grounded, and pulverized to a powdery form. The powder was passed through a 2 mm sieve. Only 200–300 g of the samples (dry—weight) was utilized for analysis due to the limited space of the detector shield.

To prevent ^{222}Radon from escaping, three different methods were adopted for sealing in each case. The sealing procedure involved coating the internal rim of the lid of the plastic container with Vaseline jelly, filling the lid assembly gap with candle wax to block the gaps between the lid and container, and tight sealing the lid container with adhesive masking tape.

The samples were then transferred to radon-impermeable cylindrical plastic containers of uniform size (70 mm height by 60 mm diameter) after weighing and were sealed for about 30 days. This was done to allow radon and its short-lived progenies to reach secular radioactive equilibrium before gamma measurements. The soil used for referencing was also transferred to a container of the same material and dimensions as were used for the fish samples. A lead-shielded 76 × 76 mm NaI(TI) detector crystal (Model No. 727 series, Canberra Inc.) that is coupled to a Canberra Series 10 plus Multichannel Analyzer (MCA) (Model No.1104) through a preamplifier was used for the radioactivity measurements. It has a resolution (FWHM) of about 8% at energies of about 662.0 keV, which is considered adequate to distinguish the gamma-ray energies of interest in this current study. The choice of gamma-ray peaks for the radionuclides to be used for measurement in this study was made considering the fact that the NaI(TI) detector used in this study had a modest energy resolution. This was to ensure that the photons emitted by the radionuclides would only be sufficiently discriminated against if their emission probability and their energy were high enough, and the surrounding background continuum low enough. Therefore, the activity concentration of ^{214}Bi (determined from the 1760 keV gamma ray peak) was chosen to

provide an estimate of 226Ra (238 U) in the samples, while that of the daughter radionuclide 208Ti (determined from its 2615 keV gamma ray peak) was chosen as an indicator of ^{208}Th (^{232}Th). ^{40}K was determined by measuring the 1460 keV gamma rays emitted during its decay. Detailed information about the gamma-spectrometry procedures can be found in our previous work (Orosun, Oniku, et al., 2020; Orosun, Usikalu, et al., 2020). The minimum detectable activity for ^{40}K, ^{238}U, and ^{232}Th was 0.0255, 0.00737, and 0.00737 Bqkg^{-1}, respectively. The fish samples were placed on the top of the detector symmetrically and measured for 29,000 seconds, which was followed by that of water and sediments. The net area under the corresponding peaks in the energy spectrum was computed by subtracting counts due to the Compton scattering of higher peaks and other background sources from the total area of the peaks.

2.5. Calibration and efficiency determinations

The system was calibrated for energy and efficiency. Two calibration point sources were used in calibrating the system, ^{137}Cs and ^{60}Co. The calibrations were done with an amplifier gain that gives 72% energy resolution for the 661.7 keV of Cs-137 and counted for 30 minutes with the spectral lines of cobalt-60 found to be 1.161 ± 0.02 MeV and 1.325 ± 0.02 MeV.

2.6. Estimation of the radiological hazard indices

2.6.1. Absorbed dose rate

The absorbed dose rate in the air due to the concentration of the activities of preexisting radionuclides potassium-40, uranium-238, and thorium-232 ($Bqkg^{-1}$) at the coastal regions was estimated using equation 1;

$$D\left(nGyh^{-1}\right) = 0.462C_u + 0.604C_{Th} + 0.041C_K$$

where C_K, $C_{u,}$ and C_{Th} are the activities of potassium-40, uranium-238, and thorium-232 in the study samples, respectively (Sugandhi et al., 2014; UNSCEAR, 2000).

2.6.2. Annual effective dose for external exposures (AED_{Ext})

The effective dose for external exposure received by a member of the public annually was estimated using the dose rates as given in the equations below.

$$\mathrm{AED_{outdoor}}\left(\mu \mathrm{Svy}^{-1}\right) = \mathrm{D_{outdoor}}\left(\mathrm{nGyh}^{-1}\right) \times 8760\mathrm{h} \times 0.7\left(\mathrm{SvGy}^{-1}\right) \times 0.2 \times 10^{-3},$$

The dose conversion factor of 0.7 $SvGy^{-1}$ and occupancy factor for indoors as 0.8 were adopted (UNSCEAR, 2000).

2.6.3. Radium Equivalent Activity Index (Ra_{eq})

The radium equivalent (Ra_{eq}) is calculated using equation 3:

$$Ra_{eq} = C_{Ra} + 1.43C_{Th} + 0.077C_K,$$

Table 1. Spectral energy windows used in the analysis

Isotope	Gamma Energy (keV)	Energy Window (keV)
R-226	1764.0	1620–1820
Th-232	2614.5	2480–2820
K- 40	1460.0	1380–1550

where C_{Ra}, C_{Th}, and C_K are the radioactivity concentration in Bq kg^{-1} of ^{226}Ra, thorium-232, and potassium-40. The average value of the Radium Equivalent Activity Index (Ra_{eq}) is 370 Bq kg^{-1} (Sugandhi et al., 2014).

2.6.4. Radiation hazard indices
Excess Lifetime Cancer Risk (ELCR)

The Excess Lifetime Cancer Risk (*ELCR*) is calculated using equation 9:

$$ELCR = AED \times DL \times RF$$

where *AED is* the Annual Effective Dose, *DL* is the mean life duration (assuming 70 years), and RF is the fatal cancer risk per Sievert assumed to be 0.05 for stochastic effects for the populace (UNSCEAR, 2000). The recommended limit for the ELCR is 3.75×10^{-3}.

2.7. Statistical analysis

The Pearson correlation analysis and the descriptive statistical analysis were carried out using **S**tatistical **P**ackage for the **S**ocial **S**ciences (SPSS). The two variables to be tested to ensure that Pearson is checked under correlation coefficients, and the results were displayed at the output viewer of the SPSS. Similarly, the descriptive statistics were analyzed using descriptive coefficients to give the desired variability of spread samples in the study area

3. Results and discussion

3.1. In situ activity concentration using Super-Spec RS-125 y- spectrometer

The statistical summary of the results of the *in situ* measured activity concentrations of uranium-238, thorium-232, potassium-40, and the gamma dose rate (*DR*) for the seashores are presented in Table 1 and 2 and Figures 3–6. The results revealed that the activities of the primordial

Table 2. The acquired field data (in-situ measurements of uranium-238, thorium-232, and potassium-40 activities)

Points	Lat. (North)	Long. (East)	Elev. (m)	^{238}U ($Bqkg^{-1}$)	^{232}Th ($Bqkg^{-1}$)	^{40}K ($Bqkg^{-1}$)
1	5.933108	5.519315	−19	0.00	2.84	71.99
2	5.932997	5.519288	−16	32.11	29.35	331.78
3	5.933073	5.519443	−13	44.46	0.00	84.51
4	5.932915	5.519445	−14	8.65	29.23	319.26
5	5.330450	5.519607	−14	28.41	20.42	131.46
6	5.932897	5.519582	−20	6.16	33.33	131.46
7	5.933080	5.519582	−15	7.41	0.81	3.93
8	5.933045	5.598950	−17	16.10	20.72	134.93
9	5.933015	5.520023	−17	53.11	46.28	37.56
10	5.932983	5.520178	−18	7.41	28.42	12.52
11	5.932855	5.520070	−16	34.58	1.22	325.32
12	5.932740	5.520125	−18	20.99	13.80	316.13
13	5.932993	5.520312	−26	0.00	38.98	75.12
14	5.933052	5.520335	−21	0.00	26.39	0.00
15	5.932777	5.520295	−21	0.00	7.31	53.21

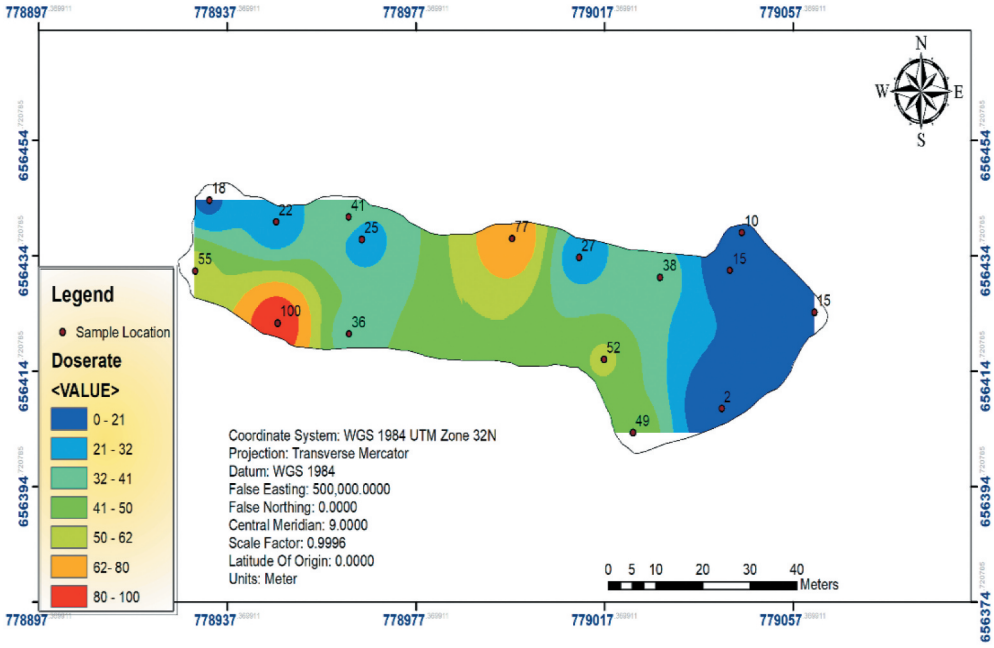

Figure 3. Spatial distribution of in-situ measured dose rate.

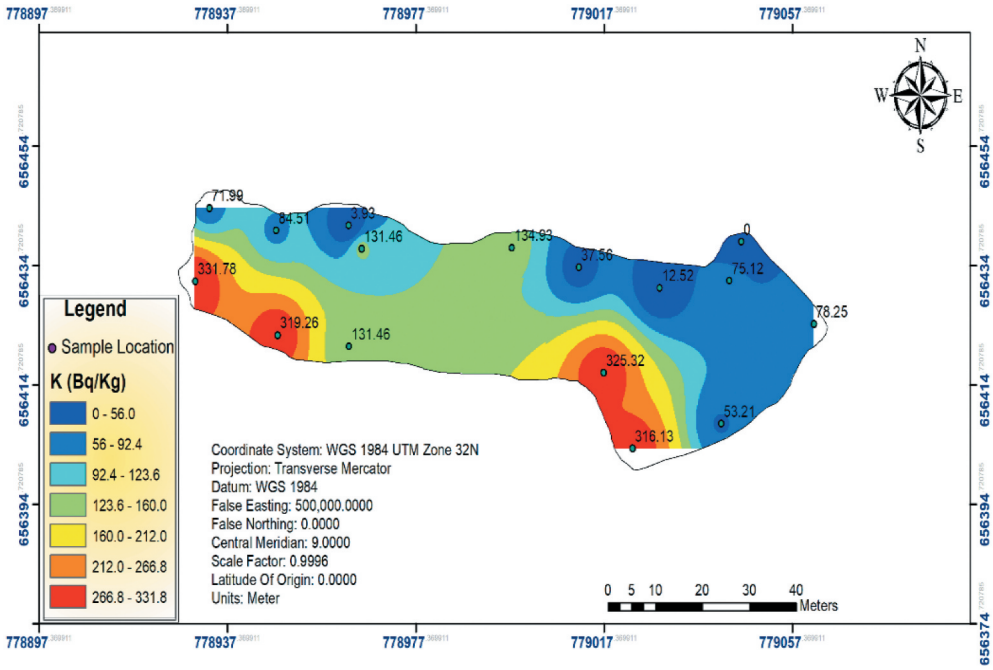

Figure 4. Spatial distribution of in-situ measured activity concentration of potassium-40.

radionuclides were skewed (having almost a symmetric distribution) since most of the measure of the asymmetry of their probability distribution about their means is in the range of −2 and +2 (Sugandhi et al., 2014). The evaluation of the coefficient of variation (CV) also discloses the variability in the distribution of the concentration of the activities at the polluted coastlines. From the results, most of the activities show high variability.

From Table 2, the lowest values of the activity concentration of potassium-40, uranium-238, and thorium-232 for the study area are below the detection limit, while their corresponding highest

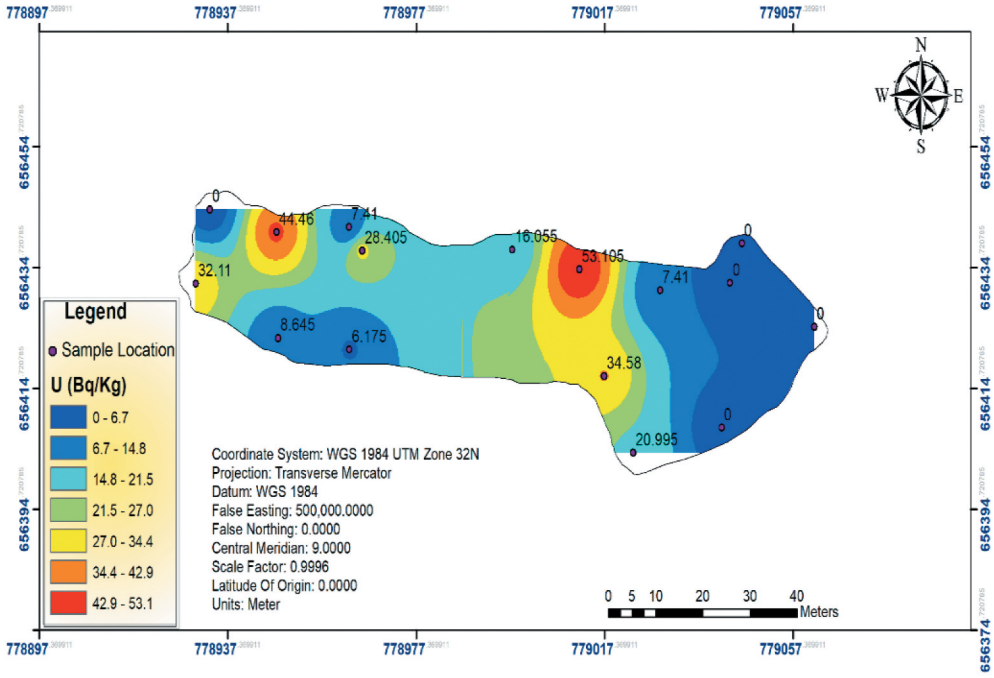

Figure 5. Spatial distribution of in-situ measured activity concentration of uranium-238.

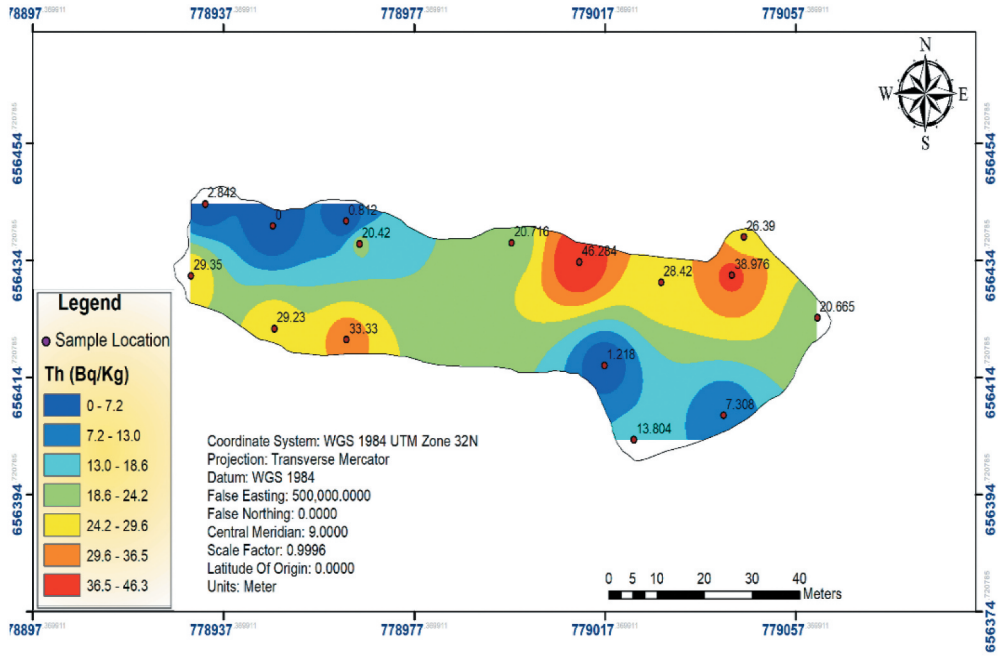

Figure 6. Spatial distribution of in-situ measured activity concentration of thorium-232.

values are 331.78, 53.11, and 46.28 $Bqkg^{-1}$, respectively. Interestingly, the highest activities of uranium-238 and thorium-232 occur at the same sampling point (i.e., location 9), which may be due to the presence of silicate sand in the sediments and the lowest values of the activities of potassium-40 and uranium-238 occur at location 14, which may be attributed to the weather/washing away of major contents of the sediments. These high and low activity concentrations of these primordial radionuclides are evident in the spatial plots using ArcGIS (Figures 3–6). The high

Table 3. Pearson correlation for the primordial radionuclides (potassium-40, uranium-238, thorium-232, and D_{out})

	^{238}U	^{232}Th	^{40}K	D_{out}
^{238}U	1.0000			
^{232}Th	0.0412	1.0000		
^{40}K	0.2883	0.0436	1.0000	
D_{out}	0.7034	0.6482	0.5003	1.0000

observed values at location 9 call for serious concern since a considerable increase in the concentration of the radionuclides increases the level of the background radiation that can lead to exposure to elevated ionization radiation levels. The estimated mean values of the in-situ measured activities of potassium-40, uranium-238, and thorium-232 are 135.28, 17.29, and 19.94 $Bqkg^{-1}$ respectively. These mean values of the activity concentration of the radionuclides are below 420.00, 32.00, and 45.00 $Bqkg^{-1}$ acceptable threshold values for exposure to potassium-40, uranium-238, and Thorium-232thorium-232, respectively, provided by (ICRP, 1991), IAEA (Radi Dar & El-Saharty, 2012) and UNSCEAR (UNSCEAR, 2000).

Table 4. Activities of potassium-40, uranium-238, and thorium-232 in the sediment samples from the coastline using 3 × 3-inch NaI(TI) gamma spectroscopy analysis

S/No.	Sample ID	Potassium-40 ($Bqkg^{-1}$)	Uranium-238 ($Bqkg^{-1}$)	Thorium-232 ($Bqkg^{-1}$)
1	S1	224.43 ± 1.3	83.47 ± 4.8	105.77 ± 2.3
2	S2	242.24 ± 1.5	75.00 ± 0.4	47.66 ± 2.0
3	S4	106.13 ± 1.9	54.90 ± 2.1	76.24 ± 1.0
4	S3	184.53 ± 1.3	60.89 ± 1.1	109.46 ± 0.8
5	S5	252.70 ± 1.9	80.63 ± 1.5	84.69 ± 1.3
6	S7	194.72 ± 2.6	72.76 ± 2.7	79.58 ± 0.1
7	S9	137.61 ± 2.4	76.24 ± 0.1	136.12 ± 0.5
8	S8	259.02 ± 1.4	71.84 ± 2.0	76.59 ± 2.8
9	S6	239.93 ± 2.3	58.25 ± 1.9	103.21 ± 2.3
10	S11	280.31 ± 0.9	96.50 ± 1.2	104.86 ± 1.9
11	S10	288.09 ± 2.5	57.30 ± 1.6	92.09 ± 2.8
12	S12	116.14 ± 1.2	59.24 ± 0.1	132.12 ± 0.2
13	S14	182.72 ± 3.0	65.52 ± 1.8	66.72 ± 1.2
14	S13	190.21 ± 1.5	54.25 ± 1.6	103.21 ± 1.3
15	S15	102.23 ± 1.0	83.44 ± 1.0	104.87 ± 1.9
16	S_Control	91.34 ± 0.1	46.23 ± 0.0	37.09 ± 0.1
	Min	102.23 ± 1.0	54.25 ± 1.6	47.66 ± 2.0
	Max	288.09 ± 2.5	96.50 ± 1.2	136.12 ± 0.5
	Mean	200.07	70.02	94.88
	Standard Error	16.10	3.27	6.10
	Median	194.72	71.84	103.21
	Mode	#N/A	#N/A	103.21
	STDV	62.34	12.67	23.61
	Variance	3885.89	160.44	557.71
	Kurtosis	−1.14	−0.56	0.05
	Skewness	−0.31	0.48	−0.10
	Range	185.86	42.25	88.47

Pearson correlation analysis was done performed to further investigate the connection between these measured radionuclides and the in-situ measured outdoor gamma dose rate. The results of the correlation analysis, which is presented in Table 3, were classified according to the correlation coefficient R (IAEA, 1996; Sugandhi et al., 2014), i.e. $0.7 \leq |R| \leq 1$ indicates a strong correlation; $0.5 \leq |R| \leq 0.7$ suggests a significant correlation; $0.3 \leq |R| \leq 0.5$ reveals a weak correlation; and $|R| < 0.3$ indicates an insignificant correlation.

(1) $\leq |R| \leq 1$ indicates a strong correlation;

(2) $\leq |R| \leq 0.7$ suggests a significant correlation;

(3) $\leq |R| \leq 0.5$ reveals a weak correlation; and

$|R| < 0.3$ indicates an insignificant correlation.

A strong correlation exists between uranium-238 and D_{out} ($R = 0.7034$), and a significant correlation was observed between thorium-232 and D_{out} ($R = 0.6482$) and between potassium-40 and D_{out} ($R = 0.5003$). However, an inconsequential correlation was observed to exist between the primordial radionuclides. The correlation results confirm that the enhanced outdoor dose rates at coastal sediments were caused mainly by uranium-238, followed by thorium-232 and then potassium-40 as shown in Table 3

3.2. Activities of potassium-40, uranium-238, and thorium-232 in the sediment, water, and fish samples from the coastline using a 3 × 3-inch NaI(TI) detector

The statistical summary of the results of the measured activity concentrations of uranium-238, thorium-232, and potassium-40 in the sediments, waters, and fishes from the sediment seashores is presented in Tables 3 to 5 and Figures 7–9. The results revealed a similar distribution observed in the in-situ measurements, i.e., the activities of the primordial radionuclides were skewed (having a symmetric distribution) since most of the measure of the asymmetry of their probability distribution about their means is in the range of −2 to +2 (Sugandhi et al., 2014). From Tables 4 and 5, the minimum values of the activity concentration of potassium-40, uranium-238, and thorium-232 for sediments and waters from the study area are 102.23, 54.24, and 47.65 $Bqkg^{-1}$ and 126.71, 39.43, and 60.24 BqL^{-1}, respectively, while their highest values are 288.09, 96.49, and 136.12 $Bqkg^{-1}$ and 257.307, 66.93, and 96.57 BqL^{-1}, respectively. This high radioactivity level in

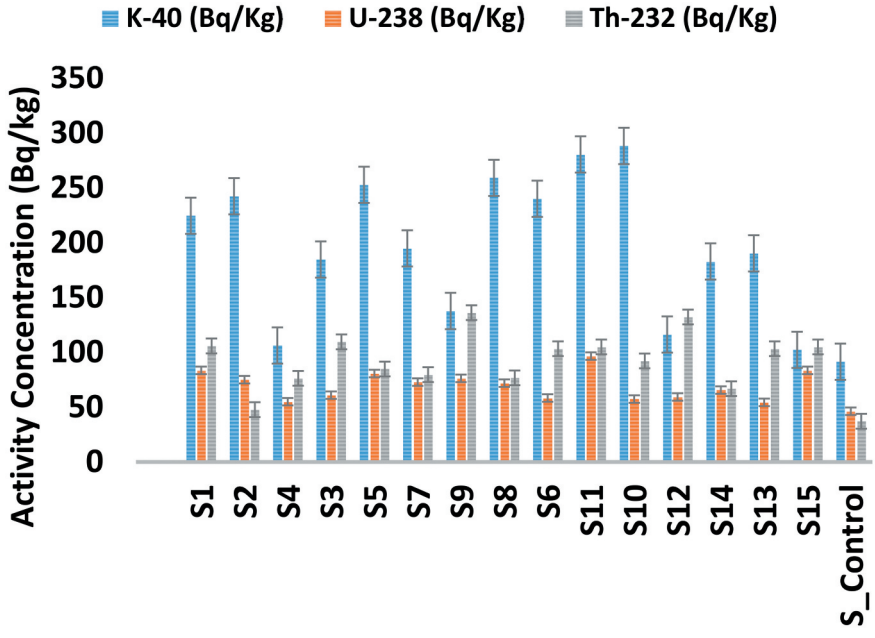

Figure 7. Activity concentration of potassium-40, uranium-238, and thorium-232 in the sediment samples.

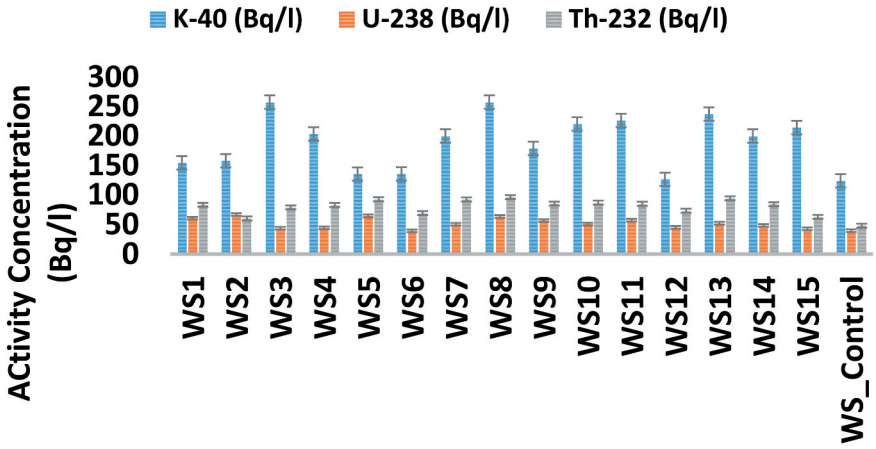

Figure 8. Activity concentration of potassium-40, uranium-238, and thorium-232 in the water samples.

water might be triggered by the chemistry of the hydrocarbon/oil spillage in the aqueous phase or due to the high contents of the drilling fluids used in oil explorations in the region. The estimated mean values of these measured activities of potassium-40, uranium-238, and thorium-232 for the sediment and water are 200.07, 70.02, and 94.88 $Bqkg^{-1}$ and 193.73, 52.59, and 82.00 BqL^{-1}, respectively. The mean values of the activity concentration of potassium-40 for both sediment and water were observed to be below the recommended level of 420.00 $Bqkg^{-1}$, whereas the average activities of uranium-238 and thorium-232 for both sediment and water were detected to be way above their corresponding global average values of 32.00 and 45.00 $Bqkg^{-1}$, respectively (Gu et al., 2017; Omeje, Adewoyin, et al., 2018; and UNSCEAR, 2000). These differences may be a result of sediment deposition underlying the study area, which is controlled by the geology of the area. The activity concentrations of these primordial radionuclides are displayed in Figures 7 and 8.

From Table 6 and Figure 9, the mean concentration of the primordial radionuclides varies from one species of fish to another. The highest mean concentrations of potassium-40 and uranium-238 were observed in Catfish with 151.87 and 38.00 $Bqkg^{-1}$, respectively, whereas the highest mean activity of thorium-232 was observed in Tilo with 89.02 $Bqkg^{-1}$. Differences in the eating habits and metabolism of the fishes are believed to be the cause of these variations. It is well known that metabolic activity and feeding habits are one of the most important factors that play an important role in toxic element accumulation in aquatic animals (Orosun et al., 2016).

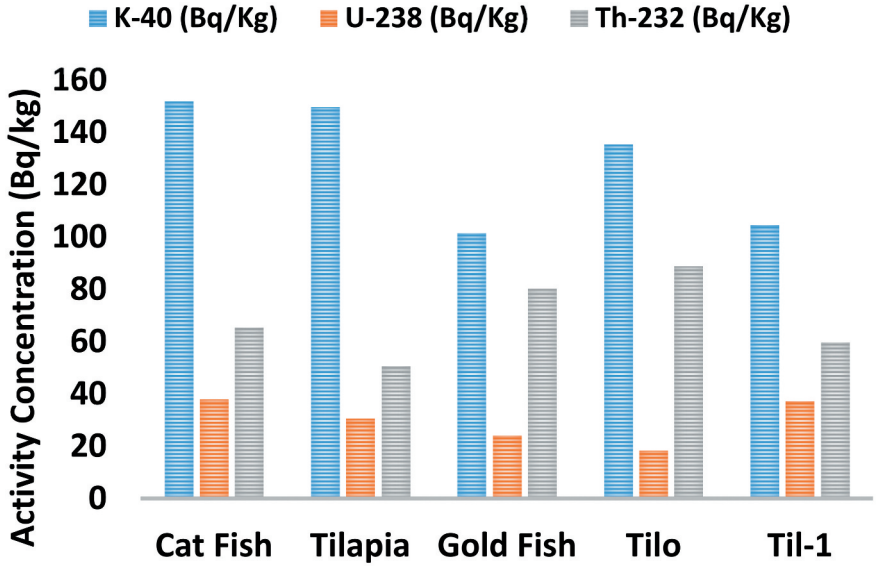

Figure 9. Activity concentration of potassium-40, uranium-238, and thorium-232 in the Fish samples.

Table 5. Activities of potassium-40, uranium-238, and thorium-232 in the water samples from the coastline using 3 × 3-inch NaI(TI) gamma spectroscopy analysis

S/No.	Sample ID	Potassium-40 (BqL^{-1})	Uranium-238 (BqL^{-1})	Thorium-232 (BqL^{-1})
1	WS1	154.61 ± 2.8	60.81 ± 2.1	83.55 ± 2.2
2	WS2	158.15 ± 1.6	66.93 ± 1.6	60.24 ± 1.1
3	WS3	257.31 ± 2.1	43.79 ± 2.1	78.95 ± 0.8
4	WS4	203.41 ± 0.5	44.59 ± 1.4	83.12 ± 1.7
5	WS5	135.52 ± 2.5	64.65 ± 2.9	92.67 ± 0.1
6	WS6	135.73 ± 1.7	39.44 ± 0.4	69.36 ± 3.1
7	WS7	200.09 ± 1.6	50.54 ± 2.1	92.48 ± 1.6
8	WS8	257.31 ± 2.1	63.69 ± 1.1	96.57 ± 2.1
9	WS9	178.85 ± 1.3	56.94 ± 2.4	85.36 ± 2.0
10	WS10	220.25 ± 2.4	50.98 ± 1.9	87.09 ± 3.8
11	WS11	226.42 ± 2.4	57.46 ± 0.9	85.24 ± 0.8
12	WS12	126.71 ± 1.4	45.17 ± 0.6	73.32 ± 3.8
13	WS13	237.30 ± 2.1	52.32 ± 1.1	94.51 ± 2.0
14	WS14	200.00 ± 1.4	48.54 ± 2.0	84.45 ± 1.1
15	WS15	214.24 ± 2.0	42.92 ± 1.8	63.08 ± 3.0
16	WS_Control	123.81 ± 0.1	39.65 ± 1.0	48.13 ± 1.0
	Min	126.71	39.44	60.23
	Max	257.31	66.93	96.57
	Mean	193.73	52.59	82.00
	Standard Error	11.27	2.26	2.87
	Median	200.09	50.98	84.45
	Mode	257.30	#N/A	#N/A
	STDV	43.60	8.75	11.10
	Variance	1900.71	76.48	123.29
	Kurtosis	−1.18	−1.21	−0.30
	Skewness	−0.14	0.24	−0.73
	Range	130.59	27.49	36.33

Table 6. Activities of potassium-40, uranium-238, and thorium-232 in the fish samples from the coastline using 3 × 3-inch NaI(TI) gamma spectroscopy analysis

S/No.	Sample ID	Potassium-40 ($Bqkg^{-1}$)	Uranium-238 ($Bqkg^{-1}$)	Thorium-232 ($Bqkg^{-1}$)
1	Catfish	151.87 ± 0.1	37.10 ± 1.4	65.51 ± 0.8
2	Tilapia	149.78 ± 0.8	30.61 ± 1.1	50.72 ± 1.3
3	Goldfish	101.57 ± 2.3	24.25 ± 2.9	80.37 ± 1.2
4	Tilo	135.41 ± 2.4	18.38 ± 1.6	89.02 ± 1.6
5	Til-1	104.79 ± 1.3	37.32 ± 2.0	59.77 ± 1.9

3.3. Evaluation of the in-situ radiological hazard indices for the coastal environment

The radiological hazard indices were estimated to evaluate the radiological risks for the coastal environment. The hazard parameters calculated are presented in Table 7. While the outdoor absorbed dose (D_{out}) rate was obtained through the in-situ measurement using the RS-125 gamma spectrometer, the indoor absorbed dose rate (D_{in}) was estimated using equation 2, and

Table 7. In-situ radiological hazard indices for the study area

	Din ($nGyh^{-1}$)	D_{out} ($nGyh^{-1}$)	AED ($mSvy^{-1}$)	Ra_{eq} ($Bqkg^{-1}$)	H_{ext}	ELCR × 10^{-3}
1	8.89	4.67	0.01	9.61	0.03	0.15
2	88.37	46.17	0.06	99.63	0.27	1.52
3	47.66	24.01	0.03	50.97	0.14	0.82
4	65.65	34.74	0.04	75.03	0.20	1.13
5	59.11	30.85	0.04	67.73	0.18	1.01
6	52.86	28.37	0.03	63.96	0.17	0.91
7	8.02	4.07	0.00	8.87	0.02	0.14
8	48.35	25.46	0.03	56.07	0.15	0.83
9	102.77	54.03	0.07	122.18	0.33	1.76
10	39.08	21.10	0.03	49.01	0.13	0.67
11	59.18	30.05	0.04	61.37	0.17	1.02
12	59.79	31.00	0.04	65.08	0.18	1.03
13	48.88	26.62	0.03	61.52	0.17	0.84
14	29.03	15.94	0.02	37.74	0.10	0.50
15	12.30	6.60	0.01	14.55	0.04	0.21
Min	8.02	4.07	0.01	8.87	0.02	0.14
Max	102.77	54.03	0.07	122.18	0.33	1.76
Mean	48.66	25.58	0.03	56.22	0.15	0.84
Std Err	6.97	3.64	0.00	8.01	0.02	0.12
Median	48.88	26.62	0.03	61.37	0.17	0.84
Std Dev	26.98	14.09	0.02	31.04	0.08	0.46
Variance	727.78	198.48	0.00	963.33	0.01	0.21
Kurt	0.03	0.10	0.10	0.44	0.43	0.03
Skew	0.18	0.18	0.18	0.25	0.25	0.18
CV	55.44	55.08	55.08	55.21	55.17	55.44
Range	94.75	49.96	0.06	113.31	0.31	1.63

the resulting values were used to evaluate the annual effective doses. The maximum and minimum values of the outdoor and indoor absorbed dose rates were observed in location 9 with 54.03 and 102.77 nGy/h and location 1 with 4.07 and 8.02 nGy/h, respectively. Expectedly, this location 9 corresponds to the location of high activities of uranium-238 and thorium-232. This means that the risk associated with exposure to ionizing radiation is high for this location. The mean values of the outdoor and indoor absorbed dose rates are 25.58 and 48.88 nGy/h, respectively. These mean values are considerably lower than the global average values of 59.00 and 84.00 nGy/h provided by UNSCEAR (UNSCEAR, 2000). Similarly, the highest and lowest outdoor and indoor annual effective dose values were observed in location 9 with 0.07 and 0.50 mSv/y, and location 1 with 0.01 and 0.04 mSv/y, respectively. The mean values calculated for the outdoor and indoor annual effective doses (0.03 and 0.24 mSv/y, respectively) are within the global average values of 0.07 and 0.41 mSv/h for outdoor and indoor exposures, respectively.

The estimated values for the *ELCR* corroborated our earlier findings with location 9 and location recording the maximum and minimum values, respectively. Fortunately, the mean values estimated for all the hazard indices are within their corresponding recommended limits.

Table 8. Radiological hazard indices for sediments and Water from the study area

Sediments						Water	
Points	**D_{in} ($nGyh^{-1}$)**	**D_{out} ($nGyh^{-1}$)**	**Ra_{eq} $Bqkg^{-1}$**	**AED ($mSvy^{-1}$)**	**ELCR (x 10^{-3})**	**AED ($mSvy^{-1}$)**	**ELCR (x 10^{-3})**
S1	211.09	111.65	252.00	0.14	3.62	0.2593	0.9074
S2	140.80	73.36	161.80	0.09	2.42	0.2019	0.7068
S4	142.86	75.76	172.10	0.09	2.45	0.2458	0.8604
S3	191.20	101.82	231.64	0.12	3.28	0.2533	0.8865
S5	187.56	98.77	221.20	0.12	3.22	0.2836	0.9926
S7	170.06	89.67	201.56	0.11	2.92	0.2101	0.7354
S9	230.88	123.08	281.49	0.15	3.96	0.2804	0.9816
S8	171.07	90.07	201.32	0.11	2.94	0.3018	1.0563
S6	186.32	99.09	224.33	0.12	3.20	0.2637	0.9229
S11	226.55	119.41	268.04	0.15	3.89	0.2681	0.9382
S10	177.05	93.90	211.16	0.12	3.04	0.2670	0.9344
S12	209.13	111.93	257.12	0.14	3.59	0.2227	0.7795
S14	148.29	78.06	175.01	0.10	2.55	0.2893	1.0124
S13	178.66	95.20	216.49	0.12	3.07	0.2585	0.9048
S15	200.29	106.08	241.26	0.13	3.44	0.2010	0.7036
S_Control	90.63	47.50	106.30	0.06	1.56	0.1541	0.5394
Min	140.80	73.36	161.80	0.09	2.42	0.2010	0.7036
Max	230.88	123.08	281.49	0.15	3.96	0.3018	1.0563
Mean	184.79	97.86	221.10	0.12	3.17	0.2538	0.8882

3.4. Evaluation of the radiological hazard indices for the sediments, waters, and fishes from the study area using the laboratory gamma spectroscopy analysis data

The mean AED_{ing} , which is a result of ingestion of the radionuclides in the water, is 0.2538 mSv/y. However, this mean value is less than the 1.00 mSv/y recommended by USEPA. The estimated mean values of AED *and the ELCR* for both water and fish are within the recommended limit (See Table 8). Also, Table 9 presents the radiological hazard indices for the Fish from the study area.

Table 9. Radiological hazard indices for the Fishes from the study area

Sample Type	AED_{ing} ($mSvy^{-1}$)	ELCR (x 10^{-3})
Catfish	0.2005	0.7017
Tilapia	0.1581	0.5533
Goldfish	0.2286	0.8002
Tilo	0.2505	0.8768
Til-I	0.1819	0.6366

4. Conclusions

This study reported the in-situ measurements and laboratory activity concentrations of potassium-40, uranium-238, thorium-232, and the outdoor dose rate of the study area in the Niger Delta areas of Nigeria. The in-situ measurements were consolidated with laboratory analysis of sediments, water, and fish from the same coastal region. The results revealed varying activities of the preexisting radionuclides (potassium-40, uranium-238, and thorium-232) with average values within the acceptable limits for the in-situ measurements. However, values within the global average values for the

radionuclides were recorded in the measured samples. Similarly, the radiation impact assessments reveal values that are mostly within the global average values for the in-situ and in sediments and water samples. Significantly, the estimated mean values of all the hazard indices for the measured samples are within their respective worldwide population weighted mean concentrations. This study recommended further research on soil sediments and marine water microbial and geochemical analysis to derive a comprehensive conclusion on what could be the main cause of death of fish.

Author contributions

A.G.U., O.M., A.O.O., and J.E.S. conceived and designed the research work. M.M.O., A.G.U., and U.M.R. collect the data and wrote the paper. M.M.O., G.N., and M.A.S. performed the risk analysis and final compilation of the work.

Data availability statement

The data supporting the findings of this study are available on request from the corresponding author.

Acknowledgments

The authors would like to thank the Covenant University Center for Research, Innovation, and Discovery (CUCRID) for providing enabling Environment to execute this research. In addition, we thank the Unumherin Community in Niger Delta for their assistance during the data collection. Finally, we thank the Biotechnology and Radiation Geophysics Research Cluster for their effective contributions in all aspects of this study.

Funding

The authors did not receive funding for this research.

Author details

Maxwell Omeje[1]
E-mail: maxwell.omeje@covenantuniversity.edu.ng
Godfrey Usiaka Aimua[1]
Olusegun Oladotun Adewoyin[1]
Muyiwa Michael Orosun[2]
Emmanuel Sunday Joel[3]
Mojisola Rachael Usikalu[1]
Omohinmin A. Conrad[4]
Oha I. Andrew[5]
Benjamin Nnamdi Ekwueme[6]
Nwankwo Chukwuma Michael[7]
Omeje U. Anne[8]

[1] Department of Physics, College of Science and Technology, Covenant University, Ota, Ogun, Nigeria.
[2] Department of Physics, University of Ilorin, Ilorin, Kwara, Nigeria.
[3] Department of Earth Sciences, Anchor University, Lagos, Nigeria.
[4] Department of Biological Sciences, College of Science and Technology, Covenant University, Ota, Ogun, Nigeria.
[5] Department of Geology, University of Nigeria, Enugu, Nsukka, Nigeria.
[6] Department of Civil Engineering, University of Nigeria, Enugu, Nsukka, Nigeria.
[7] Department of Computer and Information Sciences, College of Science and Technology, Covenant University, Ota, Ogun, Nigeria.
[8] Department of Community Health and Primary Care, College of Medicine, University of Lagos, Idiaraba, Lagos, Nigeria.

Disclosure statement

No potential conflict of interest was reported by the authors.

Citation information

Cite this article as: Dispersion of gamma dose rates and natural radionuclides in the coastal environments of the Unumherin community in Niger Delta, Maxwell Omeje, Godfrey Usiaka Aimua, Olusegun Oladotun Adewoyin, Muyiwa Michael Orosun, Emmanuel Sunday Joel, Mojisola Rachael Usikalu, Omohinmin A. Conrad, Oha I. Andrew, Benjamin Nnamdi Ekwueme, Nwankwo Chukwuma Michael & Omeje U. Anne, *Cogent Engineering* (2023), 10: 2204546.

References

Abbasi, A., Zakaly, H. M. H., & Badawi, A. (2021). The anthropogenic radiotoxic element of 137Cs accumulates to biota in the Mediterranean Sea. *Marine Pollution Bulletin*, *164*, 112043. https://doi.org/10.1016/j.marpolbul.2021.112043

Abbasi, A., Zakaly, H. M. H., & Mirekhtiary, F. (2020). Baseline levels of natural radionuclides concentration in sediments east coastline of North Cyprus. *Marine Pollution Bulletin*, *161*, 111793. https://doi.org/10.1016/j.marpolbul.2020.111793

Adegoke, O. S., Oyebamiji, A. S., Edet, J. J., Osterloff, P. I., & Ulu, O. K. (2017). Cenozoic foraminifera and calcareous. nannofossil biostratigraphy of the Niger Delta. In O. S. Adegoke, A. S. Oyebamiji, J. J. Edet, P. I. Osterloff, & O. K. Ulu (Eds.), *Part I: Cenozoic foraminifera biostratigraphy of the Niger Delta* ,1st ed., (pp. 386–394). Elsevier. https://doi.org/10.1016/B978-0-12-812161-0.00007-7

Ajao, E. A., & Anurigwo, S. (2002). Land-based sources of pollution in the Niger Delta, Nigeria. *AMBIO: A Journal of the Human Environment*, *31*(5), 442–445. https://doi.org/10.1579/0044-7447-31.5.442

Ananias, A., Kgabi, N., Zivuku, M., Mashauri, D., (2022). Environmental radioactivity of groundwater and sediments in the kuiseb and Okavango-Omatako basins in Namibia https://doi.org/10.1016/j.pce.2020.102911

Babatunde, B. B., Sikokia, F. D., Avwiric, G. O., & Chad Umorehc, W. E. (2019). Review of the status of radioactivity profile in the oil and gas producing areas of the Niger Delta region of Nigeria. *Journal of Environmental Radioactivity*, *202*, 66–73. https://doi.org/10.1016/j.jenvrad.2019.01.015

Bastami, K. D., Neyestani, M. R., Shemirani, F., Soltani, F., Haghparast, S., & Akbari, A. (2015). Heavy metal pollution assessment in relation to sediment properties in the coastal sediments of the southern Caspian Sea. *Marine Pollution Bulletin*, *92*(1–2), 237–243. https://doi.org/10.1016/j.marpolbul.2014.12.035

Bonsignore, M., Manta, D. S., Sharif, E.A.A. -T., D'Agostino, F., Traina, A., Quinci, E. M., Giaramita, L., Monastero, C., Benothman, M., & Sprovieri, M. (2018). Marine pollution in the Libyan coastal area: Environmental and risk assessment. *Marine Pollution Bulletin*, *128*, 340–352. https://doi.org/10.1016/j.marpolbul.2018.01.043

d'Almeida, G., Kaki, C., & Adeoye, J. (2016). Benin and Western Nigeria offshore basins: A stratigraphic nomenclature comparison. *International Journal of Geosciences*, *7*(02), 177–188. https://doi.org/10.4236/ijg.2016.72014

Delbono, I., Barsanti, M., Schirone, A., Conte, F., & Delfanti, R. (2016). 210pb mass accumulation rates in the depositional area of the Magra River (Mediterranean Sea, Italy). *Continental Shelf*

Research, *124*, 35–48. https://doi.org/10.1016/j.csr.2016.05.010

Fallah, M., Jahangiri, S., Janadeleh, H., & Kameli, M. A. (2019). Distribution and risk assessment of radionuclides in river sediments along the Arvand River, Iran. *Microchemical Journal*, *146*, 1090–1094. https://doi.org/10.1016/j.microc.2019.02.028

Fouskas, F., Godelitsas, A., Argyraki, A., Pappa, F. K., & Tsabaris, C. (2018). Metal concentrations and radioactivity in sediments at the northern coastal zone of Ikaria Island, eastern Mediterranean. *Journal of Radioanalytical and Nuclear Chemistry*, *317*(1), 55–68. https://doi.org/10.1007/s10967-018-5843-z

Gu, Y. -G., Lin, Q., Huang, H. -H., Wang, L., Ning, J. -J., & Du, F. -Y. (2017). Heavy metals in fish tissues/stomach contents in four marine wild commercially valuable fish species from the western continental shelf of the South China Sea. *Marine Pollution Bulletin*, *114*(2), 1125–1129. https://doi.org/10.1016/j.marpolbul.2016.10.040

Hurtado-Bermúdez, S., Valencia, J. M., Rivera-Silva, J., Mas, J. L., Aparicio, I., Santos, J. L., & Alonso, E. (2019). Levels of radionuclide concentrations in benthic invertebrate species from the Balearic Islands, Western Mediterranean, during 2012–2018. *Marine Pollution Bulletin*, *149*, 110519. https://doi.org/10.1016/j.marpolbul.2019.110519

IAEA. (1996). Radiation protection and the safety of radiation sources. *International Atomic Energy Agency, Wagramerstrsse*, *5*, A1400. Vienna. Austria. IAEA-RPSR-1 Rev 1.

ICRP. (1991). Recommendations of the International Commission on Radiological Protection 1990 (ICRP) publication no. 60. *Annals of the ICRP*, *21*, 1–201.

International Association of Oil and Gas Producers (OGP), (2008). Guidelines for the Management of Naturally Occurring Radioactive Material (NORM) in the oil & gas industry. Report No 412.

Janadeleh, H., Jahangiri, S., & Kameli, M. A. (2018). Assessment of heavy metal pollution and ecological risk in marine sediments (a case study: Persian Gulf). *Human and Ecological Risk Assessment: An International Journal*, *24*(8), 2265–2274. https://doi.org/10.1080/10807039.2018.1443792

Janadeleh, H., Kameli, M. A., & Boazar, C. (2018). Seasonal variations of metal pollution and distribution, sources, and ecological risk of polycyclic aromatic hydrocarbons (PAHs) in sediment of the Al Hawizah wetland, Iran. *Human and Ecological Risk Assessment: An International Journal*, *24*(4), 886–903. https://doi.org/10.1080/10807039.2016.1277416

Jonkers, G., Hartog, F. A., Knaepen, W. A. I., Lancée, P. F. J., (1997). Characterization of NORM in the oil & gas production (E&P) industry. In: International Symposium on Radiological Problems with Natural Radioactivity in the Non-nuclear Industry, Amsterdam, The Netherlands, September.

Nour, H. E., El-Sorogy, A. S., El-Wahab, M. A., Nouh, E. S., Mohamaden, M., & Al-Kahtany, K. (2019). Contamination and ecological risk assessment of heavy metals pollution from the Shalateen coastal sediments, Red Sea. *Marine Pollution Bulletin*, *144*, 167–172. https://doi.org/10.1016/j.marpolbul.2019.04.056

Omeje, M., Adewoyin, O. O., Joel, E. S., Ehi-Eromosele, C. O., Emenike, P. C., Usikalu, M. R., Akinwumi, S. A., Zaidi, E., & Saeed, M. A. (2018). Natural radioactivity concentrations of 226 Ra, 232 Th, and K in commercial building materials and their lifetime cancer risk assessment in dwellers. *Human and Ecological Risk Assessment: An International Journal*, *24*(8), 214. https://doi.org/10.1080/10807039.2018.1438171

Omeje, M., Emmanuel, J. S., Olusegun, A. O., Cyril, E.E.O., Ifeanyi, A. T., & Embong, Z. (2018). A study of natural radioactivity in some building materials in Nigeria. *Radiation Protection Dosimetry. (Oxford Press, ScholarOne)*, 02 August 2018, ncy121. https://doi.org/10.1093/rpd/ncy121

Omeje, M., Olusegun, A., Emmanuel, S. J., Ijeh, B. I., Uchechukwu, A. O., Oluwasegun, A., Ogunrinola, E. I., Angbiandoo, M. T. T., Ifeany, A. O., & Saeed, M. A. (2020). Spatial distribution of gamma radiation dose rates from natural radionuclides and its radiological hazards in sediments along river Iju, Ogun state Nigeria. *MethodsX*, *7*, 101086. https://doi.org/10.1016/j.mex.2020.101086

Orosun, M. M., Oniku, A. S., Adie, P., Orosun, O. R., Salawu, N. B., & Louis, H. (2020). Magnetic susceptibility measurement and heavy metal acid at an automobile station in Ilorin, North-Central Nigeria. *Environmental Research Communications*, *2*(1), 015001. https://doi.org/10.1088/2515-7620/ab636a

Orosun, M. M., Tchokossa, P., Orosun, R. O., Akinyose, F. C., & Ige, S. O. (2016). Determination of selected heavy metals and human health risk assessment in fishes from Kiri Dam and River Gongola, Northeastern Nigeria. *Journal of Physical Chemistry & Biophysics*, 6, 229. https://doi.org/10.4172/2161-0398.1000229

Orosun, M. M., Usikalu, M. R., Oyewumi, K. J., & Achuka, J. A. (2020). Radioactivity levels and transfer factor for granite mining field in Asa, North-central Nigeria. *Heliyon*, *6*(6), e04240. https://doi.org/10.1016/j.heliyon.2020.e04240

Papaefthymiou, H., Papatheodorou, G., Moustakli, A., Christodoulou, D., & Geraga, M. Natural radionuclides and 137Cs distributions and their relationship with sedimentological processes in Patras Harbour, Greece. (2007). *Journal of Environmental Radioactivity*, *94*(2), 55–74. Powell, B.A., Hughes, L.D., Soreefan, A.M., et al., 2007. https://doi.org/10.1016/j.jenvrad.2006.12.014

Pappa, F. K., Tsabaris, C., Ioannidou, A., Patiris, D. L., Kaberi, H., Pashalidis, I., Eleftheriou, G., Androulakaki, E. G., & Vlastou, R. (2016). Radioactivity and metal concentrations in marine sediments associated with mining activities in Ierissos Gulf, North Aegean Sea, Greece. *Applied Radiation and Isotopes*, *116*, 22–33. https://doi.org/10.1016/j.apradiso.2016.07.006

Pates, J. M., & Mullinger, N. J. (2007). Determination of 222Rn in fresh water: Development of a robust method of analysis by α/β separation liquid scintillation spectrometry. *Applied Radiation and Isotopes*, *65*(1), 92–103. https://doi.org/10.1016/j.apradiso.2006.06.006

Radi Dar, M. A., & El-Saharty, A. A. (2012). Some radioactive-elements in the coastal sediments of the Mediterranean Sea. *Radiation Protection Dosimetry*, *153*(3), 361. https://doi.org/10.1093/rpd/ncs104

Savvaidis, I. (2001). Bacterial indicators and metal ions in high mountain lake waters. *Microbial Ecology in Health and Disease*, *13*(3), 147–152. https://doi.org/10.1080/089106001750462696

Sugandhi, S., Joshi, V. M., & Ravi, P. (2014). Studies on natural and anthropogenic radionuclides in sediment and biota of Mumbai Harbour Bay. *Journal of Radioanalytical and Nuclear Chemistry*, *300*(1), 67–70. https://doi.org/10.1007/s10967-014-2944-1

Tang, J., Zhang, J., Ren, L., Zhou, Y., Gao, J., Luo, L., Yang, Y., Peng, Q., Huang, H., & Chen, A. (2019).

Diagnosis of soil contamination using microbiological indices: A review on heavy metal pollution. *Journal of Environmental Management*, *242*, 121–130. https://doi.org/10.1016/j.jenvman.2019.04.061

Tiphaine, M., Pierre, C., Tiphaine, C., Paco, B., Christophe, B. -P., Sandrine, B., Emmanuelle, R., & Marc, B. (2018). Trace metal concentrations in the muscle of seven marine species: Comparison between the Gulf of Lions (North-West Mediterranean Sea) and the Bay of Biscay (North-East Atlantic Ocean). *Marine Pollution Bulletin*, *135*, 9–16. https://doi.org/10.1016/j.marpolbul.2018.05.051

Uluturhan, E., Kontas, A., & Can, E. (2011). Sediment concentrations of heavy metals in the Homa Lagoon (Eastern Aegean Sea): Assessment of contamination and ecological risks. *Marine Pollution Bulletin*, *62*(9), 1989–1997. https://doi.org/10.1016/j.marpolbul.2011.06.019

UNSCEAR, (2000): Sources and effects of ionization radiation. https://www.unscear.org/docs/publications/2000/UNSCEAR_2000_Report_Vol.I.pdf. (Retrieved on May 19, 2021).

Wang, Y. L., Wang, Q., Yuan, R., Sheng, X. F., & He, L. Y. (2018). Isolation and characterization of mineral-dissolving bacteria from different levels of altered mica schist surfaces and the adjacent soil. *World Journal of Microbiology & Biotechnology*, *35*(1), 2–13. https://doi.org/10.1007/s11274-018-2573-x

Zakaly, H. M. H., Uosif, M. A. M., Issa, S. A. M., Tekin, H. O., Madkour, H., Tammam, M., El-Taher, A., Alharshan, G. A., & Mostafa, M. Y. A. (2021). An extended assessment of natural radioactivity in the sediments of the mid-region of the Egyptian Red Sea coast. *Marine Pollution Bulletin*, *171*, 112658. https://doi.org/10.1016/j.marpolbul.2021.112658

Zaqoot, H. A., Aish, A. M., & Wafi, H. N. (2018). Study on heavy metal pollution in Gaza fishing harbour along the Mediterranean Sea-Gaza beach. *Journal of Aquatic Science and Marine Biology*, *1*, 24–34.